Engineering and Technology Journal
Journal homepage: https://etj.uotechnology.edu.iq

# Synthesized of GaN Nanostructure Using 1064 nm Laser Wavelength by Pulsed Laser Ablation in Liquid

**Husam Aldin A. Abdul Amir, Makram A. Fakhri*, Ali. A. Alwahib**

Laser and Optoelectronic Engineering Dept., University of Technology-Iraq, 10066 Baghdad, Iraq
*Corresponding author Email: makram.a.fakhri@uotechnology.edu.iq

## HIGHLIGHTS

- High-quality GaN nanofilm was prepared by pulsed laser ablation in ethanol.
- A new, thin, layer-by-layer preparation factor of GaN nanofilm was used.
- The structural properties showed a high and sharp peaks of the hexagonal GaN nanostructure and identical to the conventional structure of the GaN crystal.
- The optical properties showed an increase in the reflectivity of the gallium nanoparticles in the UV recovery.
- The increase in the optical bandgap energy showed a blueshift related to the size of the GaN nanoparticles grown on a porous silicon substrate.

## ARTICLE INFO

**Handling editor:** Ivan A. Hashim

**Keywords:**
Gallium nitride; Deposition by pulse laser ablation; X-Ray Diffraction; AFM;FESEM; Reflectance; Energy band gap

## ABSTRACT

GaN nanostructure was Synthesized using Pulsed laser ablation in liquid ethanol with Nd:YAG laser at pulsed laser ablation energy of 1600 mj and laser wavelength of 1064 nm. The nanoparticle was deposited using the drop cast method on the prepared porous silicon substrate. The structural and optical properties of the prepared GaN were studied. XRD pattern shows a high and sharp peak of pSi peak at 2θ =28.74 reflected from (111) plane and exhibits h-GaN rise at 2θ =34.54, 2θ =37.49, 2θ= 48.19 and 2θ=57.99 which are reflected from (002), (100), (102), (110) planes respectively where (002) plane has the highest peak than others. AFM and FESM proved an increase in the grain size of GaN. The reflectance of GaN (81.79%) at the wavelength (306nm) and has an energy band gap of (3.9eV).

## 1. Introduction

In recent years, nanostructured substances are very interesting compared to their bulk compared to their different physical features [1, 2]. Gallium nitride (GaN) Nanoparticles (NPs) has been recognized as the most promising material for optoelectronic and electronic applications [3, 4], due to its vast range of 3.4 eV at ambient temperature and exciting binding energy of 26 meV. Therefore, high-purity GaN nanoparticles are critical for constructing devices because of their use as active regions to create color-tunable light-emitting diodes and laser diodes [5].

Furthermore, they are valuable materials for fabricating short-wavelength electroluminescence devices due to features such as high breakdown field and carrier mobility, high temperature, chemical stability, and their relative stability even in harsh environments [6]. Due to these qualities, thin films have become one of the essential materials in industrial equipment. The following are examples of technologies: solar cells [7], pH sensors [8], light-emitting diode (LED) [9], shorter wavelength optical devices [10], high-power transistor devices [11], and beta-voltaic devices [12]. Several successful trials have attempted to synthesize GaN nanostructures using various growing techniques, including organic chemical vapor deposition of the metal [13], Reactive Epitaxial of Molecular Beam [14], Thermal Ammonia [15], Physical Vapor Deposition [16], Chemical Vapor Deposition (CVD) [17], Sol-gel Chemistry [18], Electrochemical Deposits [19], Thermal Vapor Deposition, combustion method [20], Pulsed Laser Deposition [21] and Pulsed Laser Ablation in Liquid (PLAL) [22].



http://doi.org/10.30684/etj.v40i2.2271
Received 3 July 2021; Accepted 17 September 2021; Available online 25 February 2022
2412-0758/University of Technology-Iraq, Baghdad, Iraq

The (PLAL) technique is a new technology extensively researched over the last decade, creates nanoparticles by laser ablation in liquids.

In this study, high purity of gallium netride nanostructures were prepared using a simple and cheap method, where p-type gallium nitride wafer was immersed in ethanol and shoted with tattoo removal laser pulses to prepare a gallium netride nanoparticles suspended in ethanol and then using the drop casting method on porous silicon substrates and from Then the physical properties of the prepared nanostructures were studied for using to fabricate an optoelectronics and photonic devices and various sensors.

## 2. Experimental work

The GaN target was immersed in 5ml ethanol and shot using Nd:YAG pulsed laser, as shown in Figure 1(a). Laser parameters were correctly indicated by wavelength (1064 nm) and frequency (4 Hz). One sample was prepared at energy of 1600 mg. The sample was irradiated with 500 pulses to saturate the liquid with nanomaterial. The focal length was 12 cm varying after every 100 pulses to keep the laser and the GaN surface interaction in the same manner. Figure 1(b) shows the liquid sample after the ablation method by Nd:YAG pulsed laser.

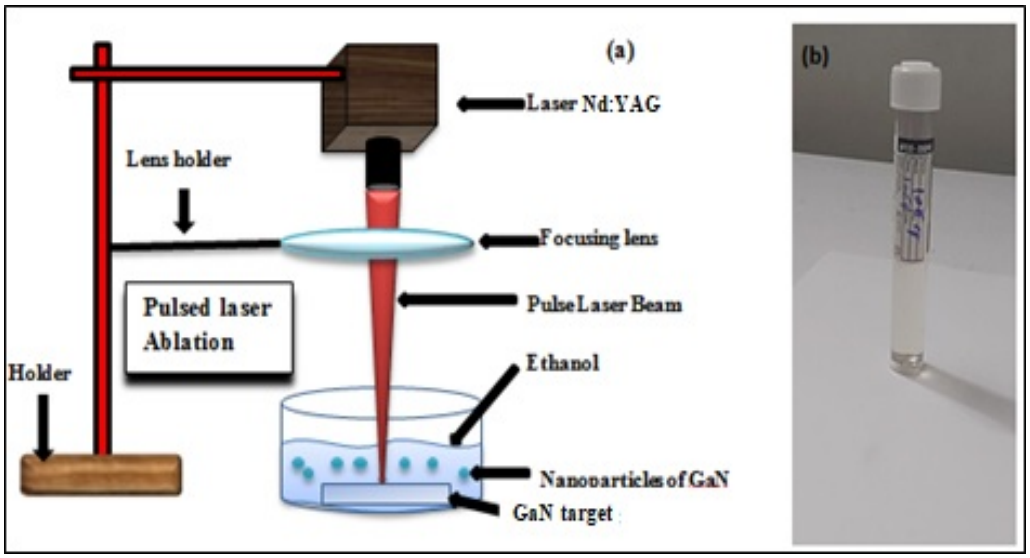


**Figure 1:** a) Laser ablation method b) liquid sample generated from ablation method at the wavelength (1064 nm)

The Photo electrochemical etching process was used to create porous Silicon. The first step was cleaning N-type Si wafer (111) using alcohol to eliminate contaminants. Silicon wafer was fixed inside the Teflon container which was filled with 20 ml of the HF (48%) solution. 30 mW diode laser working at a wavelength of 650 nm and a gold rod were applied in the experiment. The Gold rod was connected to the negative part of a DC power supply and the positive part to the Teflon base through the metal side. Gold rod immersed in the HF solution generating a current equal to 60 mA. Ten minutes of laser exposure was enough to form perfect porous Silicon. Figure 2 depicts the electro-photochemical etching process.

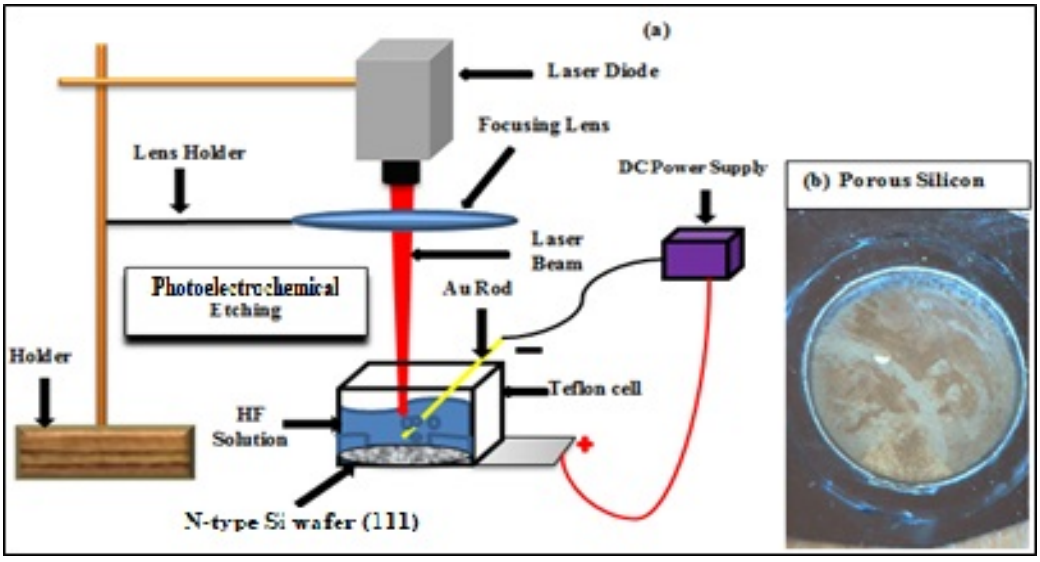


**Figure 2:** a) The photo electrochemical etching process b) Porous Silicon

Figure 3 shows the drop-casting method used to deposit GaN liquid samples on the porous silicon type-n (111) substrate. A hot plate was used to heat the porous silicon substrate to a temperature between (70°C - 90°C). When the Silicon substrate reached the desired temperature, the GaN liquid starts dropping slowly on the porous silicon substrate; each drop was allowed to dry before being followed by another fall. One hundred drops were the number to build all the GaN thin films on the porous silicon substrate. The operations were completed in less than 12 hours to avoid oxidation. The Nano-liquid should be thoroughly agitated before each drop to ensure that the GaN nanoparticles are distributed uniformly throughout all samples.

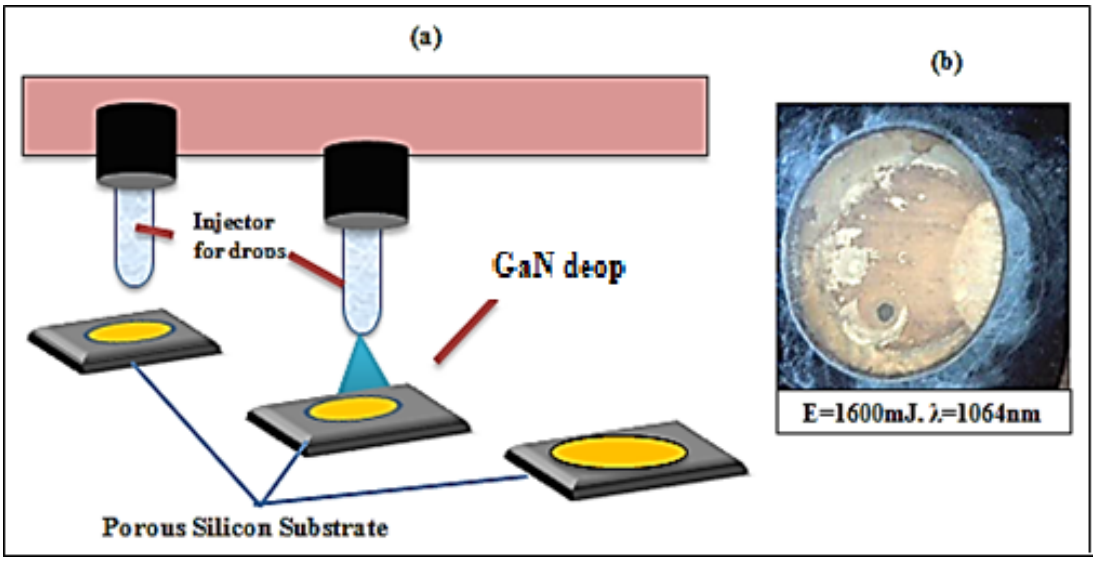


**Figure 3:** a) The drop-casting method b) GaN/ Porous Silicon-n (111) thin-film at the wavelength (1064nm)

In the next section, XRD, AFM, and FESEM were used to analyze GaN/ Porous Silicon-n (111) samples

## 3. Results and Discussion

### 3.1 Structural properties

Figure 4 (a, b) presents the XRD results of Nano porous Silicon and GaN Nanostructure. The GaN nanoparticles were ablated using 1064 nm Laser in ethanol and drop-casted on the prepared porous silicon substrate. Figure 4a shows the porous silicon XRD patterns at 2θ =28.74 reflected from the (111) plane; it offers a high and sharp peak. Figure 4b present the GaN nanostructure prepared for 1600mj at the wavelength of 1064nm exhibit hexagonal GaN rise at 2θ =34.54, 2θ =37.49, 2θ= 48.19 and 2θ=57.99 which are reflected from (002), (100), (102), (110) planes respectively; Plane111 was shown cut off due to its very high height, which affects the appearance of other planes clearly and it is refers to Si substrate, it shows an apparent disparity in the height of the peaks and the one that reflected from (002) plane has the highest peak than others. The result of X-ray diffraction also proved the success of growing gallium nitride on the used substrates, with high efficiency and purity. The mountains in the XRD pattern of diffraction are matched with the conventional GaN hexagonal structure [20].

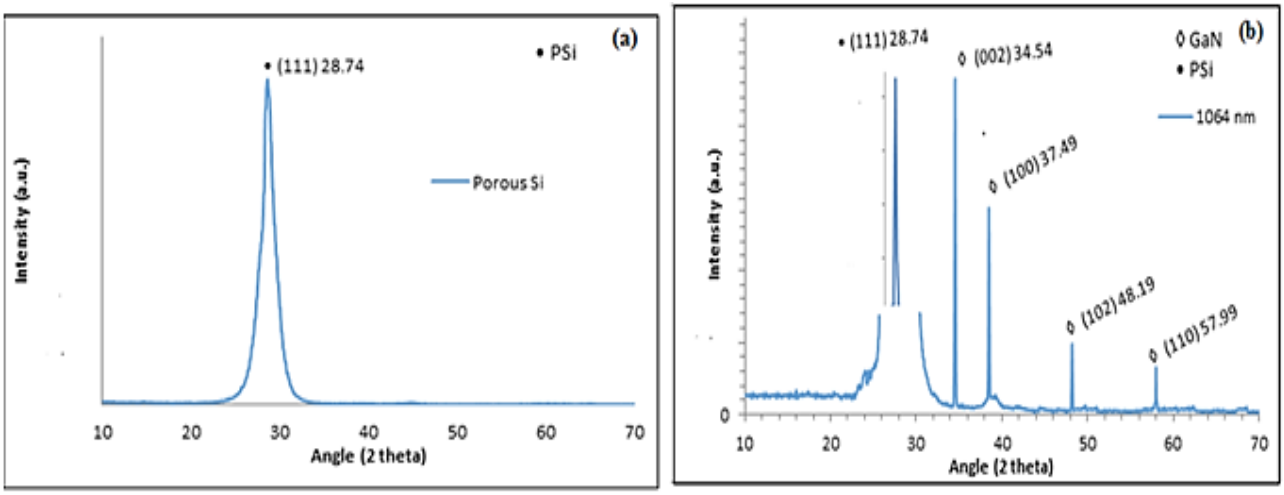


**Figure 4:** XRD patterns of a) the porous Silicon, b) GaN Nano photonics at the wavelength (1064 nm)

## 3.2 Morphological properties

### 3.2.1 AFM results

Figure 5 presents AFM images of the porous Silicon and GaN Nano photonics that were processed at the wavelength of (1064 nm). The grain size, roughness, and root mean square could be changing as shown in Table I, which exhibits porous Silicon with grain size (53.40nm), roughness (6.649 nm) and root mean square (8.925nm). Figure 5b shows GaN Nano photonics at the wavelength of (1064 nm) with grain size of (132.1 nm), roughness of (21.55 nm), and root mean square of (25.08 nm). The results show an increase in the grain size, roughness and root mean square. As shown in the surface topography of GaN Nano photonics by the AFM micrographs, the grain is distributed uniformly across the scanning area (78nm ~78nm), and each column grain is upward. The results of the topographical examination also showed an increase in the values of the roughness and particle size after the process of trituration and growth of the Nano-Gallium nitride, and this is to fill the surface pores of the porous silicon with gallium nitride granules, which were distilled over the surface of the porous silicon. This corresponds to the results previously presented [23, 24].

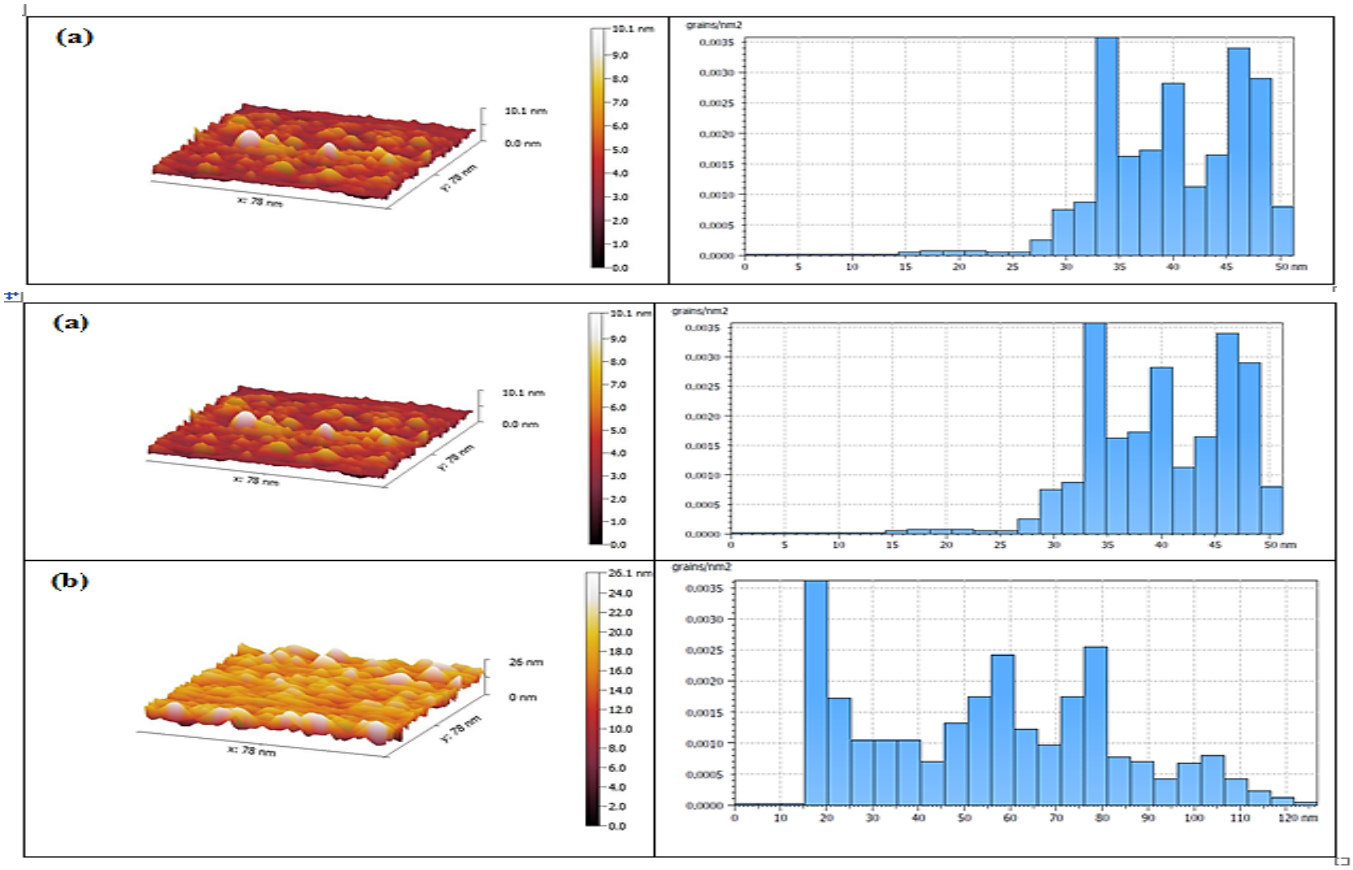


**Figure 5:** AFM images of a) the porous silicon b) GaN/pSi nanostructures at the wavelength (1064 nm)

**Table 1:** AFM data of the porous Silicon and the GaN/pSi nanostructures at the wavelength (1064nm)

| Group no | Roughness (nm) | Root-mean-square value (nm) | Grain size (nm) |
|---|---|---|---|
| pSi | 6.649 | 8.925 | 53.40 |
| GaN/pSi | 21.55 | 25.08 | 132.1 |

### 3.2.2 FESEM results

Figure 6 presents the FESEM images and the EDX spectrum of porous Silicon and GaN/pSi nanoparticles for the wavelength (1064 nm). The GaN nanoparticle was built using a drop cast on the prepared porous silicon substrate. Figure 6a shows FESEM image for the porous Silicon's surface where the pore is observed, and the EDX spectrum exhibits a high peak of Si and a tiny oxygen peak. Figure 6b exhibits the FESEM image of GaN/pSi nanoparticle where the grain size appears larger than in the porous Silicon. The EDX spectrum shows that [Ga]/[N] ratio was 4.39; the FESEM investigation proved the AFM results. This corresponds to the results previously presented [25, 26].

## 3.3 Optical results

Figure 7 presents the UV–vis spectra of the optical reflectance for the porous silicon and GaN nanoparticles grown on a porous silicon substrate at the wavelength of (1064 nm) with a range of wavelengths around 300–900 nm. Figure 7a present that

the average values of the reflectance in the ultraviolet light region decreases with the wavelength and increase in the regions of near-infrared light, and visible, and has the highest peak of reflectance in the wavelength (842 nm) that has a reflectance of (7.5%). Figure 7b shows that the average optical reflectance in the ultraviolet light region increases with the wavelength and decrease in the regions of near-infrared light and visible, and has two peaks. The first one is the highest. It represents the GaN nanoparticles with a reflectance of (81.79%) at the wavelength (306 nm). The second one represents the porous Silicon with a reflectance of (66.84%) at the wavelength (506 nm). The reflectance values of the GaN nanoparticles are related to the grain size of GaN nanoparticles grown on porous silicone substrates at wavelength (1064 nm), and supported by the AFM-FESEM analysis results were also higher in the GaN nanoparticles than in pSi. This corresponds to the results previously presented [27].

Figure 8 presents the Nanostructure's optical bandgap energy of pSi substrates and GaN nanostructure grown on a porous silicon substrate at the (1064 nm) wavelength. The energy band gap of the pSi and GaN nanostructures was calculated using the Kubelka-Munk (K-M) function and Taut plots. F(R), where R is the reflectance, was employed in the K-M formula, as illustrated in Eq. (1).

$$F_{KM} = \frac{(1-R^2)}{2R} \quad (1)$$

where R refers to reflectance.

Figure 8a shows that pSi substrates have an optical energy band gap of (2.1eV). Figure 8b exhibit that GaN nanostructure was grown on a porous silicon substrate at the wavelength of (1064 nm) has two energy band gap the first one for pSi with (2.1eV). The second one is for GaN nanostructure with an energy band gap of (3.4 eV). The results show that the optical energy band gap increases in GaN Nanostructure and the wavelength have a blue shift. This shift is related to the grain sizes. It is also supported by the AFM and FESEM results. This corresponds to the results previously presented [28].

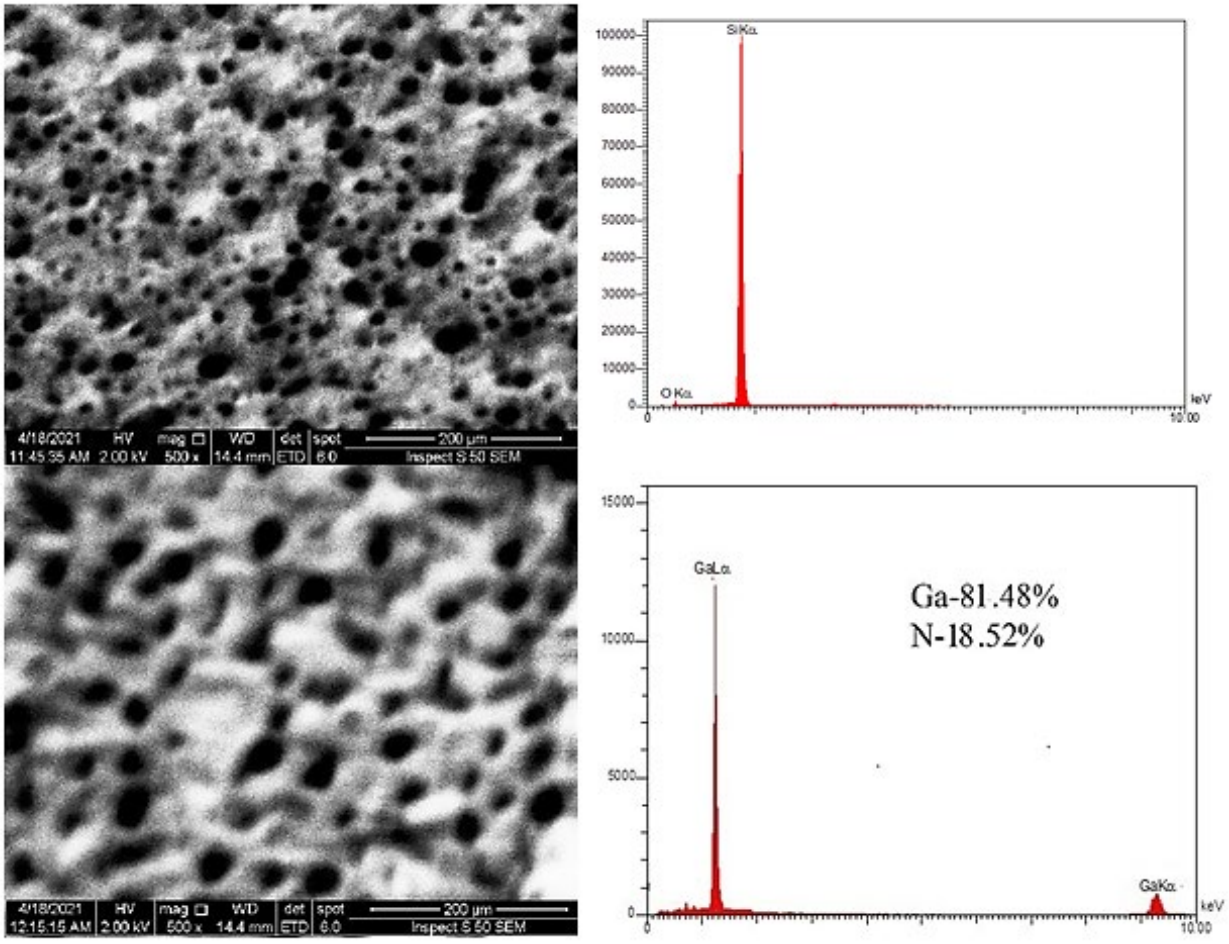


**Figure 6:** The FESEM images and EDX spectra of a) the porous silicon b) GaN nanostructures Grown on a porous silicon substrate at the wavelength of (1064 nm)

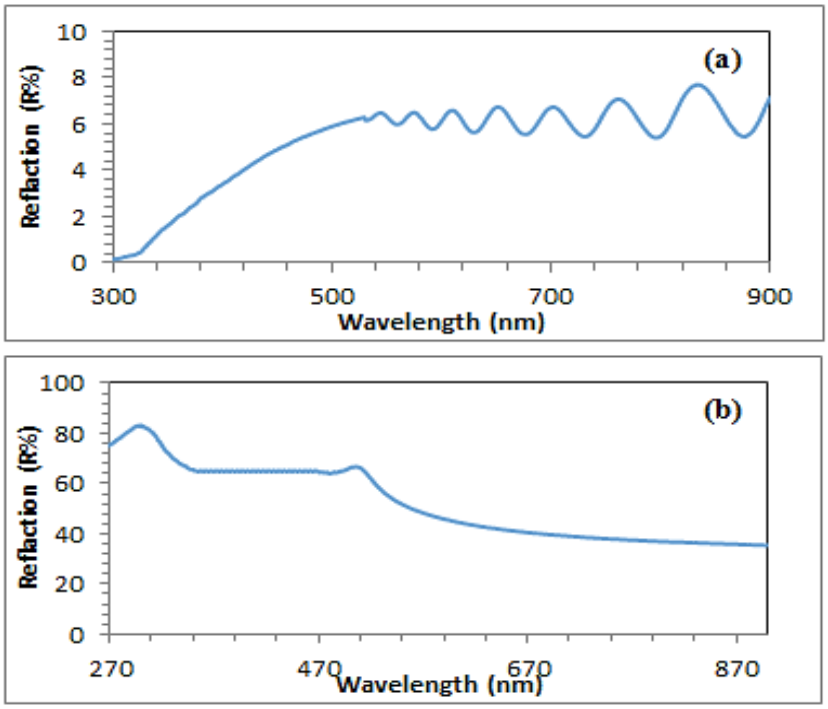


**Figure 7:** Reflectance diagram of (a) pSi substrates and (b) GaN nanostructure grown on a porous Silicon substrate at the wavelength of (1064nm)

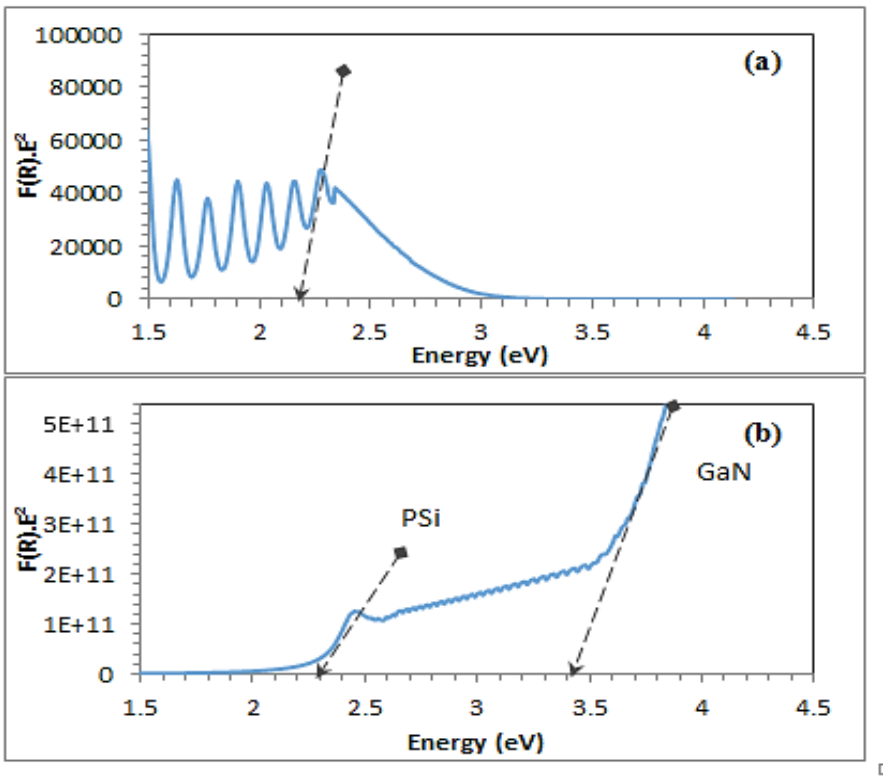


**Figure 8:** Optical energy band gap diagram of (a) pSi substrates and (b) GaN nanostructure grown on 30. A porous silicon substrate at the wavelength of (1064 nm)

## 4. Conclusions

The GaN nanoparticle was deposited using the drop cast method on the prepared porous silicon substrate. The structural properties show a high and sharp peak of hexagonal-GaN Nanostructure at three different planes and matched with the conventional GaN hexagonal structure of the GaN crystal. The topographical and surface results of the prepared Nano films showed high homogeneity, uniform distribution of nanoparticles, as well as an increase in the grain size and surface roughness due to crystal growth on the porous walls of the porous silicon. The optical properties exhibit an increase in the reflectance of

the GaN nanoparticles in the ultraviolet regain. An increase in the optical band gap energy and the wavelength will have a blue shift related to the grain size of GaN nanoparticles grown on a porous silicon substrate at the wavelength of (1064 nm). It is also supported by the AFM and FESEM results.

## Author contribution

All authors contributed equally to this work.

## Funding

This research received no specific grant from any funding agency in the public, commercial, or not-for-profit sectors.

## Data availability statement

The data that support the findings of this study are available on request from the corresponding author.

## Conflicts of interest

The authors declare that there is no conflict of interest.

## References

**[1]** R. S. Devan, R. A. Patil, J. Lin, Y. Ma, One-dimensional metal-oxide nanostructures: recent developments in synthesis, characterization, and applications, Adv. Funct. Mater., 22 (2012) 3326–3370. https://doi.org/10.1002/adfm.201201008

**[2]** N. K. Hassan , M. R. Hashim, Flake-like ZnO nanostructures density for improved absorption using electrochemical deposition in UV detection, J. Alloys. Compd., 577 (2013) 491–497. https://doi.org/10.1016/j.jallcom.2013.06.010

**[3]** K. M. A. Saron, M. R. Hashim, M. A. Qaeed, K. Al-heuseen, N. G. Elf dill, The excellent spontaneous ultraviolet emission of GaN nanostructures grown on silicon substrates by thermal vapor deposition, Mater. Sci. Semicond. Process. 29 (2015) 106–111. https://doi.org/10.1016/j.mssp.2013.11.007

**[4]** L. Pang , K. K. Kim, Improvement of Ohmic contacts to n-type GaN using a Ti/Al multi-layered contact scheme, Mater. Sci. Semicond. Process. 29 (2015) 90–94. https://doi.org/10.1016/j.mssp.2013.10.011

**[5]** M. Z. B. M. Yusoff, Z. Hassan, H. A. Hassan, M. J. Abdullah, M. Rashid, Pn-Junction photodiode based on GaN grown on Si (111) by plasma-assisted molecular beam epitaxial, Mater. Sci. Semicond. Process., 16 (2013) 1859–1864. https://doi.org/10.1016/j.mssp.2013.07.015

**[6]** M. A. Qaeed, K. Ibrahim, K. M. A. Saron, M. S. Mukhlif, A. Ismail, N. G. Elfadill, K. M. Chahrour, Q. N. Abdullah, K. S. A. Aldroobi, New issue of GaN nanoparticles solar cell, Curr. Appl. Phys., 15 (2015) 499–503. https://doi.org/10.1016/j.cap.2015.02.001

**[7]** M. Miyoshi, T. Tsutsumi, T. Kabata, T. Mori, T. Agawam, Effect of well layer thickness on quantum and energy conversion efficiencies for InGaN/GaN multiple quantum well solar cells, Solid. State. Electron., 129 (2017) 29–34. https://doi.org/10.1016/j.sse.2016.12.009

**[8]** Y. Dong, D. Son, Q. Dai, J. Lee, C. Won, J. Kim, S. Kang, J. Lee, D. Chen, H. Lu, R. Zhang, Y. Zheng, AlGaN/GaN heterostructure pH sensor with multi-sensing segments, Sensors Actuators B Chem., 260 (2018) 134–139. https://doi.org/10.1016/j.snb.2017.12.188

**[9]** A. Mantarc, Structural, Morphological, and Optical Characterization of GaN/p-Si Thin Films for Various Argon Flow Rates, JOM 'J. Met. Mater. Miner. Soc., 72 (2020) 552–560. https://doi.org/10.1007/s11837-019-03878-x

**[10]** E .M .Guerrero, C. Adelmann, F. Chabuel, J. Simon, N. T. Pelekanos, G. Mula, B. Daudin, G. Feuillet, H. Mariette, Self-assembled zinc blende GaN quantum dots grown by molecular-beam epitaxial, Appl. Phys. Let., 77 (2000) 809–811. https://doi.org/10.1063/1.1306633

**[11]** J. M. Lee, B. G. Min, C. W. Ju, H. K. Ahn, J. W. Lim, High temperature storage test and its effect on the thermal stability and electrical characteristics of AlGaN/GaN high electron mobility transistors, Curr. Appl. Phys., 17 (2017) 157–161. https://doi.org/10.1016/j.cap.2016.11.014

**[12]** M. R. Khan, J. R. Smith, R. P. Tompkins, S. Kelley, M. Litz, J. Russo, J. Leathersich, F. S. Sandvik, K. A. Jones, A. Iliadis, Design and characterization of GaN p-i-n diodes for betavoltaic devices, Solid. State. Electron., 136 (2017) 24–29. https://doi.org/10.1016/j.sse.2017.06.010

**[13]** C. Saidi, N. Chaaben, A. Bchetnia, A. Fouzri, N. Sakly, B. El Jani, Growth of scandium doped GaN by MOVPE, Super lattices Microstructure., 60 (2013) 120–128. https://doi.org/10.1016/j.spmi.2013.05.010

**[14]** Y. S. Park, T. W. Kang, R. A. Taylor, Abnormal photoluminescence properties of GaN nanorods grown on Si (111) by molecular-beam epistaxis, Nanotechnol., 19 (2008) 475402. https://doi.org/10.1088/0957-4484/19/47/475402

**[15]** S. Xue, X. Zhang, R. Huang, D. Tian, H. Zhuang, C. Xue, A simple method for the growth of high-quality GaN Nano belts, Mater. Letts., 62 (2008) 2743–2745. https://doi.org/10.1016/j.matlet.2008.01.031

**[16]** K. M. A. Saron , M. R. Hashim, Broad visible emission from GaN nanowires grown on n-Si (1 1 1) substrate by PVD for solar cell application, Superlattices. Microstruct., 56 (2013) 55–63. https://doi.org/10.1016/j.spmi.2012.12.020

**[17]** Q. N. Abdullah, F. K. Yam, J. J. Hassan, C. W. Chin, Z. Hassan, M. Bououdina, High performance room temperature GaN-nanowires hydrogen gas sensor fabricated by chemical vapor deposition (CVD) technique, Int. J. Hydrog. Energy., 38 (2013) 14085–14101. https://doi.org/10.1016/j.ijhydene.2013.08.014

**[18]** A. Podhorodecki, M. Nyk, R. Kudrawiec, J. Misiewicz, J. C. Pivin, W. Streak, Optical properties of GaN nanocrystals embedded into silica matrices, Superlattices. Microstruct., 40 (2006) 533–536 . https://doi.org/10.1016/j.spmi.2006.06.004

**[19]** K. Al-Heuseen, M. R. Hashim, N. K. Ali, Synthesis of hexagonal and cubic GaN thin film on Si (111) using a low-cost electrochemical deposition technique, Mater. Letts. 64 (2010) 1604–1606. https://doi.org/10.1016/j.matlet.2010.04.043

**[20]** M. A. Qaeed, K. Ibrahim, K. M. A. Saron, A. Salhin, Cubic and hexagonal GaN nanoparticles synthesized at low temperature, SuperLattices. Microstruct., 64 (2013) 70–77. https://doi.org/10.1016/j.spmi.2013.08.015

**[21]** M. Kawwam , K. Lebbou, The influence of deposition parameters on the structural quality of PLD-grown GaN/sapphire thin films, Appl. Surf. Sci., 292 (2014) 906–914. https://doi.org/10.1016/j.apsusc.2013.12.078

**[22]** H. H. Lee, M. Bae, S.H. Jo, J. Shin, D. H. Son, C. Won, J. Lee, Differential-mode HEMT-based biosensor for real-time and label-free detection of C-reactive protein, Sens. Actuators. B Chem., 234 (2016) 316-323. https://doi.org/10.1016/j.snb.2016.04.117

**[23]** M. A. Fakhery, Study the properties of silicon nanocrystallites prepared by wet etching, Eng. Technol. J., 28 (2010) 301-306. https://doi.org/10.30684/etj.28.2.8

**[24]** E. T. Al Waisy, M. S. Al Wazny, Responsively, rise time for $Bi_2O_3$ /Si photo detector, Eng. Technol. J., 32 (2014) 33-38. https://doi.org/10.30684/etj.32.1B.5

**[25]** M. A. Fakhery, K. S. khashan , E. T. Salem, Enhanced the response time of the P-N junction Photodetector, Eng. Technol. J., 26 (2008) 423-428.

**[26]** M. S. Mohammed, R. O. Mahdi, E. T. Salim, Effect of different oxidation temperature on nano and micro TCO's thin film, Eng. Technol. J., 32 (2014) 7-14. http://dx.doi.org/10.30684/etj.32.1B.2

**[27]** M. A Fakhry, F. A. Hattab, E. K. Hamed, Laser energy effects on optical properties of titanium di-oxide prepared by reactive pulsed laser deposition, Eng. Technol. J., 30 (2012) 3104-3111. http://dx.doi.org/10.30684/etj.30.17.12

**[28]** E. T. Salim, H. H. Rashed, Laser pulses effect on the structural and optical properties of ZnO nano particles prepared by laser ablation in water, Eng. Technol. J., 32 (2014) 198-208.